Supplementary Information

Mn^{2+}-Crosslinked Dual-Adjuvant Hydrogel for Spatiotemporal Immune Activation in Lung Cancer Therapy

*Bo Yin[1, #], Qian Zhang[1, #], Shuaijun Xiao[2], Yuanyuan Bao[1], Xuanzhi Luo[1], Munaiwaier Sabier[1], Zhouping Zhao[1], Youlan Yang[2], Mengling Wu[2], Xuebo Yan[1, *], Jiong Wang[1, *]*

[1] Department of Geriatric Respiratory and Critical Care, the First Affiliated Hospital of Anhui Medical University, Hefei, 230022, China
[2] Department of General Practice, the First Affiliated Hospital of Anhui Medical University, Hefei, 230022, China

[#]These authors contribute equally to this work.
[*]Corresponding authors: E-mail: wangjiong@ahmu.edu.cn (J Wang), yanxb@mail.ustc.edu.cn (X Yan).

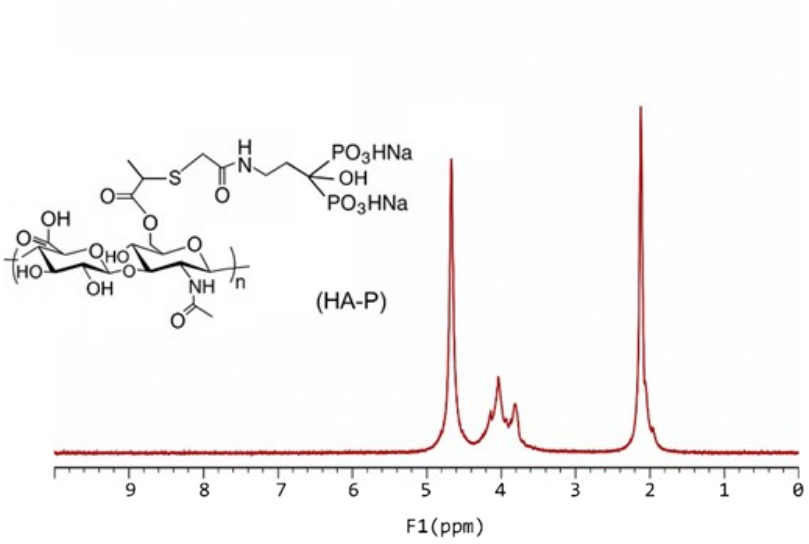

Supplementary figure 1. ^{1}H NMR spectrum of phospho-functionalized hyaluronic acid (HA-P).

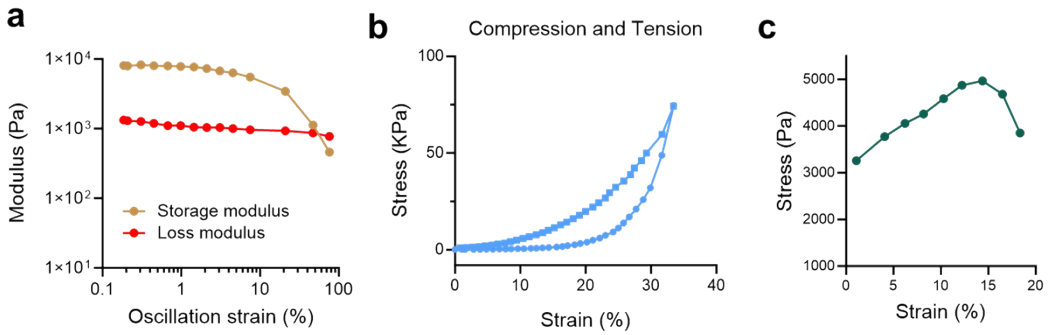

Supplementary figure 2. Mechanical characterization of CpG@Mn-Gel. (**a**) Strain-sweep rheological measurements of CpG@Mn-Gel at ω = 1 rad/s, showing storage (G′) and loss (G″) moduli as a function of oscillatory strain. (**b**) Uniaxial compressive and tensile stress–strain curves of CpG@Mn-Gel. (**c**) Tensile adhesion strength of CpG@Mn-Gel obtained from lap-shear adhesion tests.

Supplementary table 1. Gelation time of Mn2+ based hydrogels, examined by inverted vial test.

Precursor solution	Concentration of Mn^{2+}	Gelation time (s)
HA-P	50 μM	631 ± 44
HA-P	100 μM	458 ± 32
HA-P	200 μM	422 ± 26
HA-P+CpG	50 μM	665 ± 57
HA-P+CpG	100 μM	472 ± 41
HA-P+CpG	200 μM	414 ± 28

The gelation time was measured from the addition of the $MnCl_2$ solution to HA-P/HA-P+CpG solution until the gel formed no longer flowed upon vial inversion. Measurements were performed in triplicate.

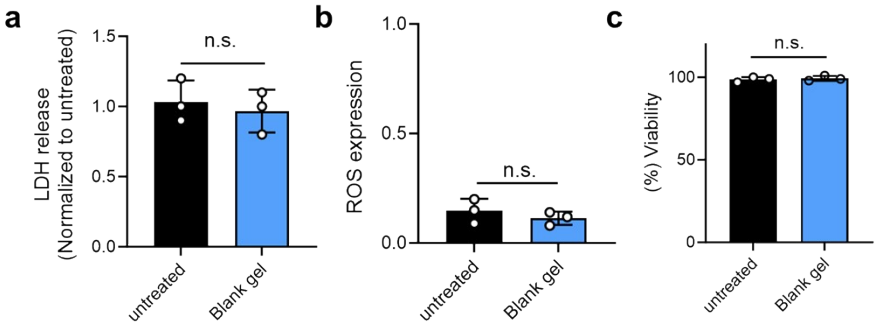

Supplementary figure 3. Tumor cells were treated with an HA hydrogel without Mn2+ (Blank Gel), and the effects on (**a**) LDH release, (**b**) intracellular ROS levels, and (**c**) cell viability were assessed.

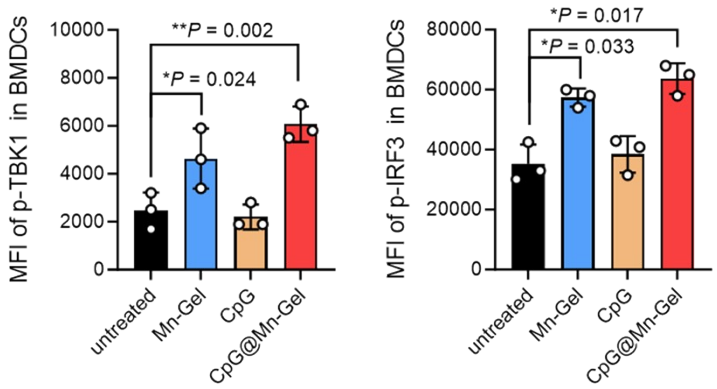

Supplementary figure 4. Flow cytometric analysis of STING pathway activation (p-TBK1 and p-IRF3) in BMDCs. Statistical significance was determined using one-way ANOVA with Tukey's post hoc test. *$P < 0.05$, **$P < 0.01$.

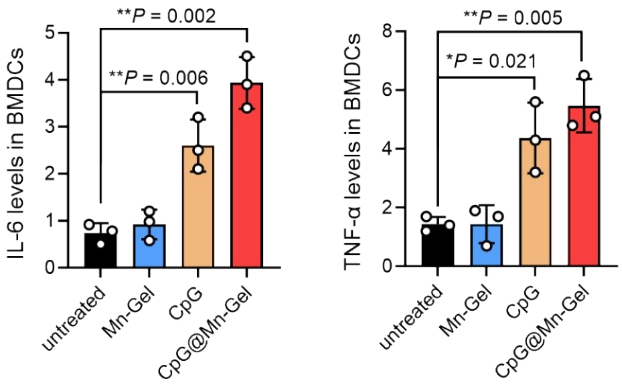

Supplementary figure 5. CpG@Mn-Gel promoted the secretion of IL-6 and TNF-α by BMDCs. BMDCs were treated with Mn-Gel, CpG, or CpG@Mn-Gel for 24 h, and the levels of IL-6 and TNF-α in the culture supernatants were quantified by ELISA (n = 3). Statistical significance was determined using one-way ANOVA with Tukey's post hoc test. *$P < 0.05$, **$P < 0.01$.

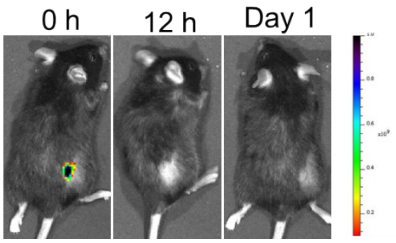

Supplementary figure 6. Degradation of subcutaneously injected free Cy5 in C57 mice.

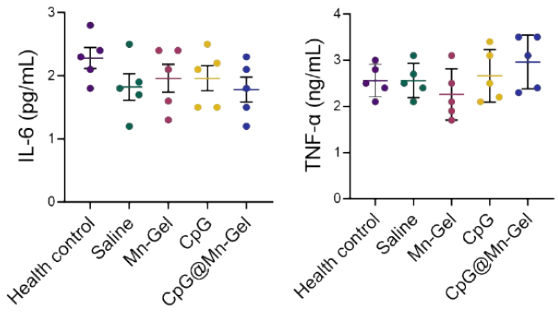

Supplementary figure 7. Serum levels of inflammatory cytokines IL-6 and TNF-α following different treatments (n = 5). Data are presented as mean ± SD.

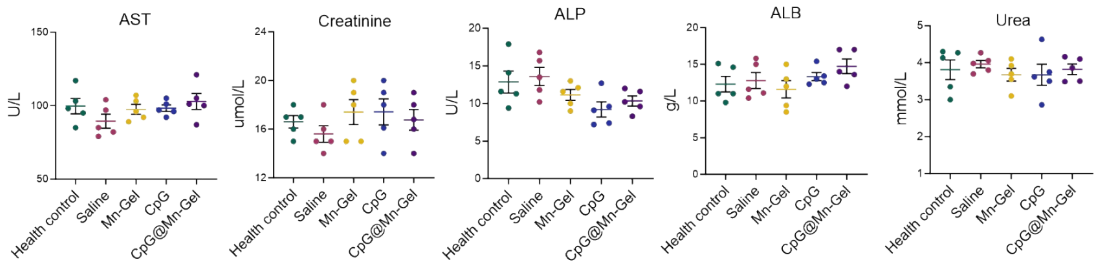

Supplementary figure 8. Assessment of liver and kidney function after different treatments. Serum biochemical indicators of hepatic and renal function including alanine aminotransferase (ALT), aspartate aminotransferase (AST), albumin (ALB), urea, and creatinine after saline, Mn-Gel, CpG, or CpG@Mn-Gel treatment (n = 5). Data are presented as mean ± SD.

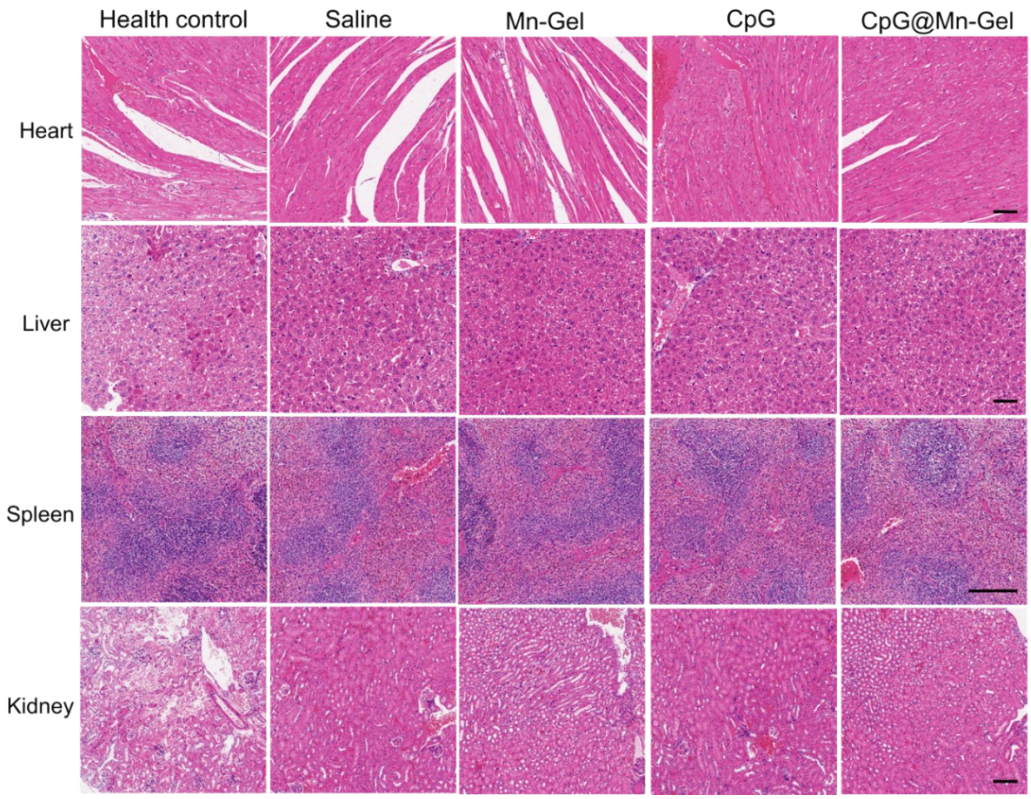

Supplementary figure 9. H&E staining for major organs (heart, liver, spleen, and kidney) in mice after various treatment. Scale bar, 100 μm.

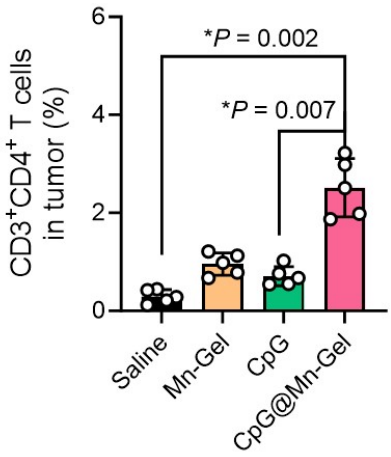

Supplementary figure 10. Flow cytometric analysis of $CD3^+CD4^+$ T cells within tumor tissues (n = 5). Statistical significance was determined using one-way ANOVA with Tukey's post hoc test. *$P < 0.05$.

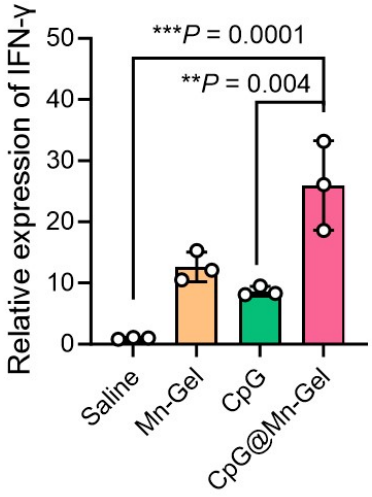

Supplementary figure 11. The relative fluorescence intensity of IFN-γ in tumor tissue (n = 3). Statistical significance was determined using one-way ANOVA with Tukey's post hoc test. *$P < 0.05$, **$P < 0.01$.